14th European Signal Processing Conference (EUSIPCO 2006), Florence, Italy, September 4-8, 2006, copyright by EURASIP

SPECTRAL CORRELATIONS AND SYNTHESIS OF MULTIDIMENSIONAL FRACTIONAL BROWNIAN MOTION

Tor Arne Øigård[a], Louis L. Scharf[b], and Alfred Hanssen[a]

[a] Department of Physics and Technology, University of Tromsø, NO-9037 Tromsø, Norway
torarne@phys.uit.no and alfred@phys.uit.no
[b] Depts. of Electrical and Computer Engineering and Statistics,
Colorado State University, Ft. Collins, CO 80523, USA
scharf@engr.colostate.edu

ABSTRACT

Fractional Brownian motions (fBm) provide important models for a wide range of physical phenomena whose empirical spectra obey power laws of fractional order. Extensions of fBm to higher dimension has become increasingly important. In this paper we study isotropic d-dimensional fBm in the framework of inhomogeneous random fields, and we derive exact expressions for the dual-wavenumber spectrum of fractional Brownian fields (fBf). Based on the spectral correlation structure of fBf we develop an algorithm for synthesizing fBf. The proposed algorithm is accurate and allow us to generate fractional Brownian motions of arbitrary dimension.

1. INTRODUCTION

Fractional Brownian motion in one dimension was introduced by Kolmogorov in 1940 and studied in the seminal paper [10] by Mandelbrot and Van Ness in 1968. It is a useful non-stationary model for certain fractal and long-range dependent processes of interest in physics, biology, finance, and telecommunications [9, 15, 24], and it is the only self-similar Gaussian process with stationary increments.

In the last few years, image processing using fractal models has represented an active research area stimulated by the plethora of applications [2] such as infographics [16], geophysics [9, 10], turbulence [1], satellite imagery, texture modeling, classification and segmentation [7, 8]. See [17] for a comprehensive tutorial on image processing using multidimensional fractal models. Natural phenomena are widely presumed to be statistical self-similar. As a consequence, natural images tend to be scale invariant – seeing an object from ten meters or one meter will result in very similar images transmitted by our visual system [11, 19], and in [23] it is shown that fractal processes provide a good model of the correlation structure of a large class of images.

Due to its wide applicability, simulation of synthetic fBm has drawn a lot of attention. Although it is possible to generate *exact* discrete-time realizations of fBm, many *approximate* methods have been proposed as alternatives to exact simulation. See [3] and references therein for extensive treatments of various methods for synthesizing fBm. Among the approximate simulation methods, *spectral techniques*, e.g. [20, 26], have become increasingly popular. The spectral methods is based on the spectral properties of fBm and generates a process that has a spectral density $S(f) \propto f^{2H+1}$. The synthesized process is first generated in the frequency-domain followed by a transformation to the time domain. However, this power law behavior of fBm in the frequency domain is a time averaged spectrum [5], and the construction of a process based entirely on this time averaged power spectrum would imply that the resulting process is an approximation to true fBm. This problem is circumvented in the spectral method by Yin [26] by simulating the *stationary increments* of fBm instead, and then the increments are integrated to form the fBm process.

It is known that non-stationary random processes have correlations between the different frequency components in the spectral domain, and that these frequency correlations are the reason for the non-stationary behavior [6, 21, 25]. In [12, 13] the spectral correlations of fBm was derived and explored, and it was shown that fBm has a very distinctive spectral correlation structure.

In this paper we derive the spectral correlation structure of *multidimensional fractional Brownian motions* or *fractional Brownian fields*, and we develop a spectral synthesizer which accounts for that particular spectral correlation structure of fBf.

2. MULTIDIMENSIONAL FBM

An *isotropic fractional Brownian field* (fBf) or *Lévy fractional Brownian field* of dimension $d \in \mathbb{N}$, is the Gaussian zero-mean field $B_H(\mathbf{x})$, $\mathbf{x} \in \mathbb{R}^d$, with temporal correlation function [17, 18]

$$\begin{aligned} R_{B_H}(\mathbf{x},\mathbf{t}) &= \mathrm{E}\{B_H(\mathbf{x})B_H(\mathbf{x}-\mathbf{t})\} && (1)\\ &= \frac{V_H}{2}\left(\|\mathbf{x}\|^{2H}+\|\mathbf{x}-\mathbf{t}\|^{2H}-\|\mathbf{t}\|^{2H}\right), && (2)\end{aligned}$$

where $0<H<1$ is the Hurst parameter, $\|\cdot\|$ is the Euclidean norm in $\mathbb{R}^d$, $\mathrm{E}\{\cdot\}$ is the statistical expectation operator, and

$$V_H = \frac{2^{1-d-2H}}{\pi^{d/2}H}\frac{\Gamma(1-H)}{\Gamma(d/2+H)}. \qquad (3)$$

Here $\mathbf{x} = (x_1,\ldots,x_d)^T$ and $\mathbf{t} = (t_1,\ldots,t_d)^T$ are two d-dimensional vectors, $x_i \in \mathbb{R}$, and T is the vector transpose.

The fractional Brownian field is an inhomogenous random field and therefore has the following spectral representation,

$$B_H(\mathbf{x}) = \int_{-\pi}^{\pi}\cdots\int_{-\pi}^{\pi} e^{j\mathbf{k}^T\mathbf{x}}dZ(\mathbf{k}), \qquad (4)$$

where $\mathbf{k}$ is a d-dimensional wavenumber vector which measures spatial frequency or wavenumber, and $dZ(\mathbf{k})$ is the

complex valued non-orthogonal infinitesimal Fourier generator (*or generalized Fourier transform*) with the following incremental spectral covariance

$$(2\pi)^{2d}\,\mathrm{E}\{dZ(\mathbf{k})dZ^*(\mathbf{k}-\mathbf{v})\} = S_{B_H}(\mathbf{v},\mathbf{k})d\mathbf{v}d\mathbf{k}. \quad (5)$$

The spectral correlation function $S_{B_H}(\mathbf{v},\mathbf{k})$ is called the *dual-wavenumber spectrum*, and this quantity describes the essential feature of inhomogenous random fields, namely that there is correlation between the different wavenumber components of $dZ(\mathbf{k})$. Conversely, a homogenous random field would have $S_{B_H}(\mathbf{v},\mathbf{k}) = S_0(\mathbf{k})\delta(\mathbf{k}-\mathbf{v})$, for some non-negative function $S_0(\mathbf{k})$, and $\delta(\mathbf{k})$ denotes Dirac's delta function. The function $S_0(\mathbf{k})$ is the conventional wavenumber spectrum, or power spectrum for $d = 1$. Thus, it is clear that for a homogenous random process, the wavenumber spectrum is a second order statistical quantity that contains all relevant spectral information. However, for inhomogenous random fields, the spectral behavior is much more complicated due to the correlations between the different wavenumber components. Hence, the dual-wavenumber spectrum must be considered when analyzing inhomogenous random fields. According to Eq. (4), we may think of $B_H(\mathbf{x})$ as a superposition of complex oscillations $\exp\left(j\mathbf{k}^T\mathbf{x}\right)$ with complex infinitesimal random amplitudes $dZ(\mathbf{k})$ that are statistically correlated for different wavenumbers.

The temporal correlation function $R_{B_H}(\mathbf{x},\mathbf{t})$ is the multidimensional inverse Fourier transform of $S_{B_H}(\mathbf{v},\mathbf{k})$ [14],

$$R_{B_H}(\mathbf{x},\mathbf{t}) = \int_{-\infty}^{\infty}\cdots\int_{\infty}^{\infty} S_{B_H}(\mathbf{v},\mathbf{k})e^{j(\mathbf{v}^T\mathbf{x}-\mathbf{k}^T\mathbf{t})}\frac{d\mathbf{v}d\mathbf{k}}{(2\pi)^{2d}}, \quad (6)$$

where the spatial vector $\mathbf{x}$ and wavenumber vector, $\mathbf{k}$ are *global* variables, while the spatial vector $\mathbf{t}$ and the wavenumber vector $\mathbf{v}$ are *local* variables.

In order to gain further insight into the inhomogenous characteristics of fBf, we may derive the dual-wavenumber spectrum of fBf by Fourier transforming $R_{B_H}(\mathbf{x},\mathbf{t})$ with respect to the temporal variables $\mathbf{x}$ and $\mathbf{t}$. However, the Fourier transform of Eq. (6) does not exist in the ordinary sense, since the integral $\int_{-\infty}^{\infty} e^{j\mathbf{k}^T\mathbf{x}}\|\mathbf{t}\|^{\alpha}d\mathbf{t}$ is divergent. By the use of Hadamard's finite part, however, one may formulate the integral transform in the sense of distribution theory [4, p. 364], to obtain the following dual-wavenumber spectrum for fBf,

$$S_{B_H}(\mathbf{v},\mathbf{k}) = 2\pi\Big[\|\mathbf{k}\|^{-(2H+1)}\delta(\mathbf{v}) - \|\mathbf{k}\|^{-(2H+1)}\delta(\mathbf{v}+\mathbf{k}) - \|\mathbf{v}\|^{-(2H+1)}\delta(\mathbf{k})\Big]. \quad (7)$$

The two-dimensional dual-frequency spectrum $S_{B_H}(v,k)$ was developed for 1D fractional Brownian motion in [12, 13], and it was shown that this spectrum provides us with a new way of interpreting the non-stationary behavior of fBm. The same interpretations is also valid for $S_{B_H}(\mathbf{v},\mathbf{k})$. For the one-dimensional case we can formulate the following interpretation of the dual-frequency spectrum. The frequency correlation is real valued, and it is represented as a line spectrum with spectral support on three discrete lines. For $v = 0$ we have the stationary manifold, so the spectrum $S_{B_H}(0,k)dk = \mathrm{E}\left\{|dZ(k)|^2\right\} = 2\pi|k|^{-(2H+1)}dk$ is the conventional stationary power spectrum. Stationary random processes would have a contribution along this line only. However, since fBm is a non-stationary random process, the dual-frequency spectrum $S_{B_H}(v,k)$ will have non-zero contributions also outside the stationary manifold. For $k = 0$, we have that $S_{B_H}(v,0)dv = \mathrm{E}\{dZ(0)dZ^*(v)\} = 2\pi|v|^{-(2H+1)}dv$ is the correlation of the DC component of the Fourier generator with all other frequency components of the Fourier generator. For $v = -k \neq 0$, $S_{B_H}(-k,k)dk = \mathrm{E}\{dZ(k)dZ^*(0)\} = 2\pi|k|^{-(2H+1)}dk$ is also a manifestation of the correlation between the DC component of the Fourier generator, and the Fourier generator for all other frequencies k. Thus, the two lines have the same interpretation, namely that the DC component of the Fourier generator is correlated with all other frequency components of the Fourier generator. Both of these lines are clearly outside the stationary manifold, and they give rise to the non-stationary behavior of fBm. Thus, we see that by only considering the power spectrum of fBm, crucial information regarding the correlation structure in the frequency domain is lost.

3. SPECTRAL SYNTHESIS OF FBF

The underlying idea of the spectral synthesis method in this section is that a prescription of the correct spectral correlation of the increment field $dZ(\mathbf{k})$ in Eq. (4), will give rise to a fractional Brownian field $B_H(\mathbf{x})$ with $0 < H < 1$. Thus, by generating samples from the $dZ(\mathbf{k})$ process with the spectral correlation structure of Eq. (7), we can use the spectral representation in Eq. (4) to construct the inhomogenous field $B_H(\mathbf{x})$.

We will organize the development of the filtering process to generate $dZ(\mathbf{k})$ in the following way. First, we construct a complex 2×1 vector containing the infinitesimal stochastic Fourier generators for the DC component and all the other wavenumbers

$$d\mathbf{Z}(\mathbf{k}) = \begin{bmatrix} dZ(\mathbf{0}) \\ dZ(\mathbf{k}) \end{bmatrix}, \quad \mathbf{k} > 0. \quad (8)$$

Then we obtain the second-order covariance matrix

$$\begin{aligned}\mathbf{R}(\mathbf{k})d\mathbf{k} &= \mathrm{E}\left\{d\mathbf{Z}(\mathbf{k})d\mathbf{Z}^H(\mathbf{k})\right\} \\ &= \begin{bmatrix} S_{B_H}(\mathbf{0},\mathbf{0}) & S_{B_H}(-\mathbf{k},\mathbf{k}) \\ S^*_{B_H}(-\mathbf{k},\mathbf{k}) & S_{B_H}(0,\mathbf{k}) \end{bmatrix}\frac{d\mathbf{k}}{(2\pi)^d}. \quad (9)\end{aligned}$$

From Eq. (9) we can, as shown in [22], build the Fourier filtering diagram shown in Fig. 1. This filter reproduces $d\mathbf{Z}(\mathbf{k})$ with the correct spectral correlation structure. We see that to generate the increment process $dZ(\mathbf{k})$ of fBf we first generate the infinitesimal Fourier generator of the white noise process, $dW(\mathbf{k})$, where

$$\mathrm{E}\left\{|dW(\mathbf{k})|^2\right\} = \frac{d\mathbf{k}}{(2\pi)^d}. \quad (10)$$

and $dW(\mathbf{k})$ is the infinitesimal Fourier generator of the d-dimensional homogeneous Gaussian random field $W(\mathbf{x})$. Then the process $dW(\mathbf{k})$ is scaled and combined such that the correlations of $d\mathbf{Z}(\mathbf{k})$ are given by Eq. (7). From the Fourier filter diagram shown in Fig. 1 we see that to obtain $dZ(\mathbf{0})$ we scale $dW(\mathbf{0})$ with a factor $\sqrt{S_{B_H}(\mathbf{0},\mathbf{0})}$, i.e.,

$$dZ(\mathbf{0}) = \sqrt{S_{B_H}(\mathbf{0},\mathbf{0})}dW(\mathbf{0}). \quad (11)$$

To obtain $dZ(\mathbf{k})$, $\mathbf{k} \neq 0$ we see that $dW(\mathbf{k})$ and $dW(0)$ are scaled and combined in the following way,

$$dZ(\mathbf{k}) = \frac{S_{B_H}(\mathbf{0},\mathbf{k})}{\sqrt{S_{B_H}(\mathbf{0},\mathbf{0})}} dW(\mathbf{0}) \qquad (12)$$
$$+\sqrt{S_{B_H}(\mathbf{0},\mathbf{k})}\left[1 - \frac{S^2_{B_H}(-\mathbf{k},\mathbf{k})}{S_{B_H}(\mathbf{0},\mathbf{0})S_{B_H}(\mathbf{0},\mathbf{k})}\right]^{1/2} dW(\mathbf{k}).$$

Finally, we build the process $B_H(t)$ from the spectral representation in Eq. (4).

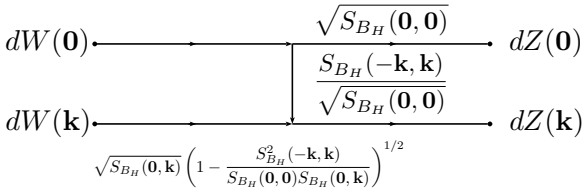

Figure 1: Filtering diagram for synthesis of fBf.

To realize this filtering diagram we need to discretize the spectral processes $dZ(\mathbf{k})$ and $dW(\mathbf{k})$. To discretize $dW(\mathbf{k})$ we integrate it over a frequency d-dimensional cube of size Ω_n

$$dW(\mathbf{k}_n) = \int_{\Omega_n} dW(\mathbf{k}), \quad n = 0,\ldots,N-1, \qquad (13)$$

with variance

$$\mathrm{Var}\, dW(\mathbf{k}_n) = \int_{\Omega_n} d\omega = |\Omega_N| = \frac{(2\pi)^d}{N}. \qquad (14)$$

Now, the Fourier generator $dW(\mathbf{k})$ is an orthogonal complex valued Gaussian field, so the discretized random field $dW(\mathbf{k}_n)$ can be generated from a complex Gaussian distribution ($\mathscr{N}_{\mathscr{C}}$), i.e., $dW(\mathbf{k}_n) \sim \mathscr{N}_{\mathscr{C}}[0,(2\pi)^d/N]$. Next, to generate the $dZ(\mathbf{k}_n)$ ($n \neq 0$), which is the discrete version of the increment process of fBf, we sample the functions $S_{B_H}(0,\mathbf{k})$ and $S_{B_H}(-\mathbf{k},\mathbf{k})$ for the wavenumbers $k_{in} = 2\pi n/N$, $i = 1,\ldots,d$, and combine them along with $dW(k_n)$ as prescribed by Eq. (12). Since

$$S_{B_H}(\mathbf{0},\mathbf{0}) = \lim_{\mathbf{k}\to\mathbf{0}} \frac{1}{\|\mathbf{k}\|^{2H+1}} \to \infty, \qquad (15)$$

we approximate the variance of the DC component of the increment process to fBf with a large but finite positive constant C^2. Regardless of the value of C, the covariance of $d\mathbf{Z}(\mathbf{k})$ is given by Eq. (9), with $S(\mathbf{0},\mathbf{0})$ replaced by C^2. Thus, even for finite C, the correlation of $dZ(\mathbf{k})$, and the cross-correlation of $dZ(\mathbf{0})$ and $dZ(\mathbf{k})$, are correct. Only the scale of $dZ(\mathbf{0})$ is approximated. A discretized version of the filtering diagram in Fig. 1 is shown in Fig. 2.

Finally, to generate the discrete fBf $B_H[\mathbf{x}]$ we take the real part of an inverse discrete Fourier transform of the discrete incremental process $dZ(\mathbf{k}_n)$, $n = 0,\ldots,N-1$.

In Fig. 3 we have implemented the spectral synthesizer in Fig. 2 for one-dimension, i.e. $d = 1$, and show synthetic fBm samples generated for different values of the Hurst parameter H. The same sample seed for the realizations of

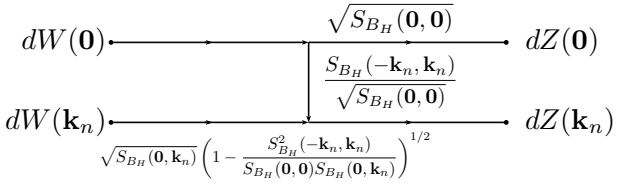

Figure 2: Filtering diagram for synthesis of discrete fBf.

the white noise increment process was used for the different values of H. The parameters were $N = 1024$, and $C = N$. For $H = 1/2$, shown in the middle panel, we have ordinary Brownian motion. In the top panel we have generated fBm samples for $H = 0.1$, and in the lower panel we have generated fBm samples for $H = 0.8$. We see that all the sample paths have the same structural shape, but for small values of H the sample path fluctuates more than ordinary Brownian motions. For larger values for H we observe that the sample path is smoother than Brownian motion.

The increment of fBm is defined as [26]

$$W_H(x) = B_H(x+\Delta x) - B_H(x),\ x \geq 0 \qquad (16)$$

and $W_H(x)$ is called fractional Gaussian noise (fGn). Since the autocovariance function characterizes a stationary Gaussian random process uniquely, insight into the performance of the spectral synthesizer can be obtained by comparing the estimated autocovariance function from the increments of the synthesized fBm data with the desired autocovariance [3]. The autocovariance function of $W_H(t)$ is given by [3, 18, 26]

$$R_{W_H}(\tau) = \frac{V_H}{2}\left(|\tau+1|^{2H} + |\tau-1|^{2H} - 2|\tau|^{2H}\right). \qquad (17)$$

In Fig. 4 we show a comparison between the true autocovariance function $R_{W_H}(\tau)$ of fGn, and the empirical sample autocovariance function $\widehat{R}_{W_H}(\tau)$ obtained from synthesized fBm for various values of H. Solid lines show $R_{W_H}(\tau)$ and dashed lines show $\widehat{R}_{W_H}(\tau)$. The estimated autocovariance function is obtained by Monte Carlo simulations where $M = 100$ realizations of length $N = 2^{14}$ was used for each value of H. Fig. 4a shows the performance of the spectral synthesizer in terms of accuracy for $H = 0.1$. We observe a close fit between the estimate $\widehat{R}_{W_H}(\tau)$ and the true value $R_{W_H}(\tau)$. The match between the sample autocovariance and the desired function is not exact, but the realizations are good approximations to fBm. This applies in general for all $H < 1/2$ for this spectral synthesizer. Fig. 4b show the performance of the spectral synthesizer in terms of accuracy for $H = 0.8$, and we see that we have a very good match between the estimate $\widehat{R}_{W_H}(\tau)$ and the true value $R_{W_H}(\tau)$. This applies in general for all $H > 1/2$. Thus, in the long-range dependent regime of fBm this spectral synthesizer produce accurate realizations of fBm.

In Fig. 5 we have implemented the spectral synthesizer in Fig. 2 for two dimensions, i.e. $d = 2$, and show synthetic fBf samples generated for different values of H. The parameters were $N = 512$ and $C = N^2$. In the upper panel we have generated an image using $H = 0.1$, in the middle we used $H = 0.5$, and in the lower panel we used $H = 0.8$. The interpretation of the Hurst parameter for images is related to the "roughness"of the fBf [17]. Small values of H yield rougher

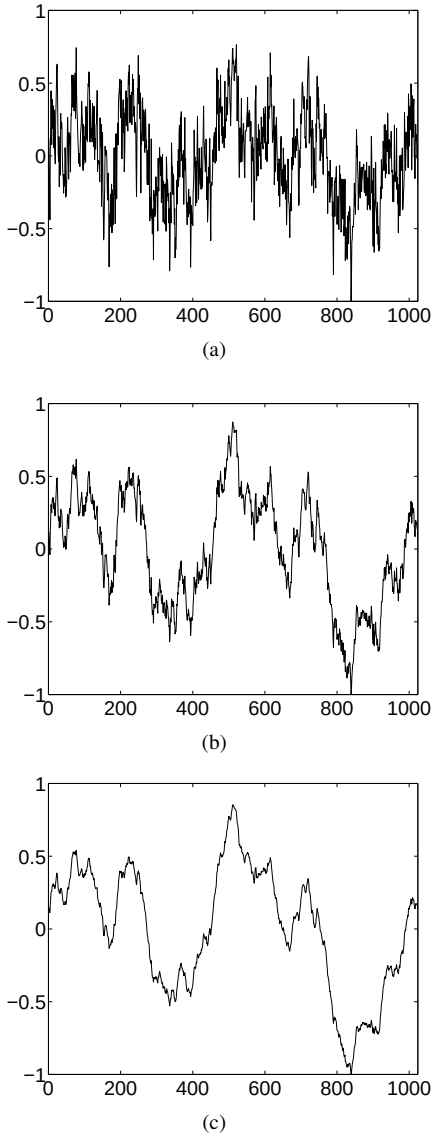

Figure 3: Synthetic fBm sample paths for (a) $H = 0.1$, (b) $H = 0.5$, and (c) $H = 0.8$. Here $N = 1024$ and $C = N$.

textures, and when H approaches 1, the smoother the corresponding texture. This effect for various values of H can be observed in Fig. 5

The degree of accuracy can be controlled by changing the frequency resolution of the stochastic Fourier generator $dW(\mathbf{k}_n)$. By increasing N we increase the accuracy of the synthesizer. The self-similarity property of fBm can be used to obtain a sample on an arbitrary equispaced grid. Numerical simulations show that the accuracy of the synthesizer also depends on the C parameter which represents the standard deviation of $d\widetilde{Z}(0)$. When $C \to \infty$ we see from Eq. (12) that the correlation between the DC component and all the other frequency components vanish, and the synthesizer converge to a spectral filter with wavenumber response $G(\mathbf{k}) = \|\mathbf{k}\|^{1-H-d/2}$ discussed in [17, 18]. Simulations show that $C = N^d$ yields good results.

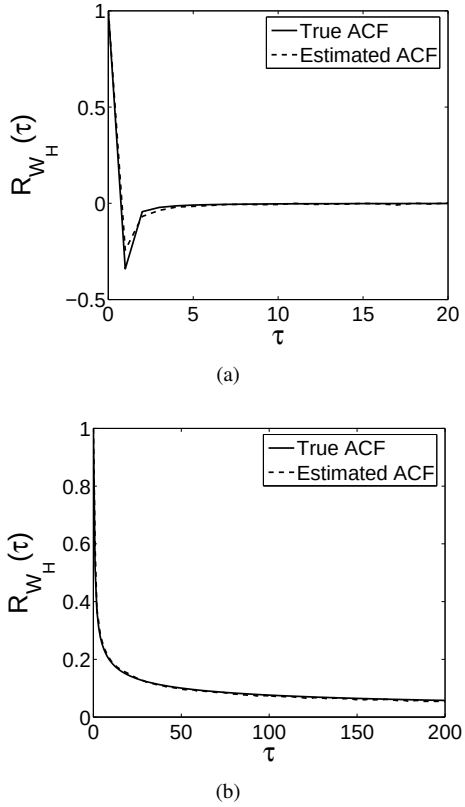

Figure 4: Comparison between the theoretical autocovariance function (ACF) of fGn and estimated autocovariance function from synthesized fGn data for (a) $H = 0.1$ and (b) $H = 0.8$.

4. CONCLUSION

In this paper we derived the dual-wavenumber spectrum for multidimensional fractional Brownian fields. This spectrum shows that fBf has a distinct spectral correlation structure, and the inhomogeneous property of fBf is caused by the particular correlation structure of this spectrum. We developed a filter based spectral synthesizer of multidimensional fractional Brownian motion. The accuracy of the synthesizer increases with increasing spectral resolution. However, as opposed to other spectral synthesizers, this synthesizer explicitly takes advantage of the inhomogeneous correlation structure of the stochastic Fourier generator of fBf. Also, the resulting process does not have a periodic behavior. Since the method applies the inverse Fast Fourier Transform, samples can be generated very fast with a high degree of accuracy. In contrast to some other methods for synthesizing fBm this method is not recursive, and it does not proceed in stages for increasing resolution.

REFERENCES

[1] P. Abry, "Ondelettes et Turbulences, Multirésolutions, algorithmes de décompositions, invariance d'échelle et signaux de pression," Diderot, Editeurs des Sciences et des Arts, Paris, 1997.

[2] M. Dekking, J. Lévy Véhel, E. Lutton, and C. Tricot,

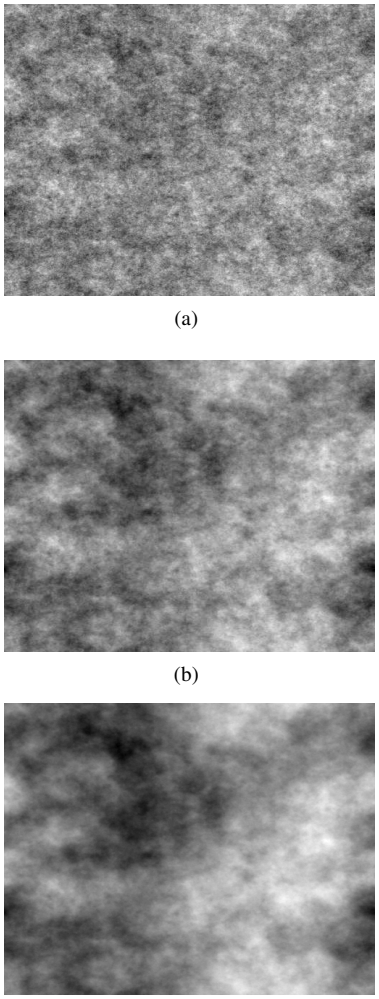

(a)

(b)

(c)

Figure 5: Synthetic 2-D fractional Brownian fields for (a) $H = 0.1$, (b) $H = 0.5$, and (c) $H = 0.8$. Here $N = 512$ and $C = N^2$.

Fractals: Theory and Applications in Engineering. New York: Springer Verlag,1999.

[3] A. B. Dieker and M. Mandjes, "On spectral simulation of fractional Brownian motion," *Probability in the Engineering and Informational Sciences*, vol. 17, pp. 417-434, 2003.

[4] I. S. Gradshteyn and I. M. Ryzhik, *Table of Integrals, Series, and Producs*

[5] P. Flandrin, "On the spectrum of fractional Brownian motions", *IEEE Transactions on information theory*, Vol. 35, 1989.

[6] A. Hanssen and L. L. Scharf, "A theory of polyspectra for nonstationary stochastic processes," *IEEE. Trans. Signal Processing*, vol. 58, pp. 327-332, 1997.

[7] J. Lévy Véhel, "Introduction to the multifractal analysis of images," in *Fractal image encoding and analysis*. Eds. Y. Fisher, Springer Verlag, 2000.

[8] J. Lévy Véhel, "Fractal approaches in signal processing," *Fractals*, vol. 3, pp. 755-775, 1995.

[9] B. B. Mandelbrot, *The Fractal Geometry of Nature*. New York: W.H. Freeman and Company, 1983.

[10] B. B. Mandelbrot and J. W. Van Ness, "Fractional Brownian motions, fractional noises and applications," *SIAM Rev.*, vol. 10, No 4, pp. 422-437, 1968.

[11] D. Mumford and B. Gidas, "Stochastic models for generic images," *Q*uarterly Appl. Math., vol. 59, pp. 85-111, 2001.

[12] T. A. Øigård, A. Hanssen, and L. L. Scharf, "Spectral correlations of fractional Brownian motion," To be submitted, 2006.

[13] T. A. Øigård, L. L. Scharf, and A. Hanssen, "Time-frequency and dual-frequency representation of fractional Brownian motion," *IEEE Workshop on Statistical Signal Processing*, France, July, 17-20, 5 pages, 2005.

[14] T. A. Øigård, L. L. Scharf, A. Hanssen, "Multivariate-Multidimensional Rihaczek spectra and accociated canonical correlations", *Third IEEE Sensor Array and Multichannel Signal Processing Workshop*, p. 547-551, Sitges, Barcelona, Spain, July 18-21, 2004.

[15] L. Pietronero and E. Toscatti, *Fractals in Physics*, Amsterdam:North-Holland, 1986.

[16] O. Peitgen and D. Saupe, Eds., *The Science of Fractal Images*. New York: Springer-Verlag, 1988.

[17] B. Pesquet-Popescu and J. Lévy Véhel, "Stochastic Fractal Models for Image Processing," *IEEE Signal Processing Magazine*, vol. 19, no. 5, pp. 48-62, 2002.

[18] I. S. Reed, P. C. Lee, and T. K. Truong, "Spectral representation of fractional Brownian motion in *n* dimensions and its properties," *IEEE Transactions on Information Theory*, vol. 41, No. 5, pp. 1439-1451, 1995.

[19] D. L. Ruderman and W. Bialek, "Statistics of natural images: Scaling in the woods," *Physical Review Letters*, vol. 73, pp. 814-818, 1994.

[20] D. Saupe, "Algorithms for random fractals", in *The Science of Fractal Images*, Eds. H.-O. Peitgen and D. Saupe, Springer-Verlag, New York, 1988.

[21] L. L. Scharf, P. J. Schreier, and A. Hanssen, "The Hilbert space geometry of the Rihaczek distribution for stochastic analytic signals," *IEEE Signal Processing Lett.*, vol. 12, pp. 297-300, 2005.

[22] L. L. Scharf and J. K Thomas, "Wiener filters in canonical coordinates for transform coding, filtering and quantizing",*IEEE Trans. Signal Processing*, Vol. 46, No. 3, pp. 647-654, 1998.

[23] S. Tirosh, D. Van De Ville, and M. Unser, "Polyharmonic smoothing splines and the multi-dimensional Wiener filtering of fractal-like signals", *IEEE Transactions on Image Processing*, In press, 2006.

[24] R. F. Voss, "Evolution of long-range fractal correlations and $1/f$ noise in DNA base sequences," *Phys. Rev. Lett.*, vol. 68, pp. 3805-3808, 1992.

[25] A. M. Yaglom, *Stationary Random Functions*. New York: Dover, 1973.

[26] Z. -M, Yin, "New methods for simulation of fractional Brownian motion," *Journal of Computational Physics*. vol. 127, pp. 66-72, 1996.